Acta Polytechnica **64**(6):501–510, 2024
https://doi.org/10.14311/AP.2024.64.0501

Published by the Czech Technical University in Prague

CO_2 CAPTURE IN PILOT-SCALE UNIT USING SOLID ADSORBENT IN BIOMASS FLUIDISED BED BOILER FLUE GAS

Michael Dvořák*, Jan Hrdlička, Lukáš Pilař, Pavel Skopec, Jiří Burda

Czech Technical University in Prague, Faculty of Mechanical Engineering, Department of Energy Engineering, Technická 4, 160 00 Praha, Czech Republic

* corresponding author: michael.dvorak1@fs.cvut.cz

Abstract. The search for methods to capture carbon dioxide (CO_2) emissions from solid fuel combustion processes has led to the development and subsequent testing of alternative innovative CO_2 capture technologies. Vacuum Pressure Swing Adsorption (VPSA) method is a promising technology for efficient CO_2 capture using solid sorbents. This article introduces CO_2 capture using the VPSA technology, providing description of the selected VPSA method and the construction of a pilot-scale unit for VPSA CO_2 capture. The main goal of this article is to present experimental results, including a description of the pilot-scale unit used for the VPSA adsorption tests using zeolite 13X, an industrially proven sorbent for CO_2 capture. The measured adsorption values were compared with theoretical isotherms, allowing the assessment of VPSA method efficiency and accuracy in practical conditions. Results indicated discrepancies between the experimental unit and the theoretical adsorption models, attributed to non-ideal conditions, non-optimised processes, incomplete drying of the sorbent, and temperature variations affecting the adsorption efficiency. The conclusion confirms the VPSA lab unit's ability to adsorb CO_2 using solid sorbents, suggesting that further research and additional tests with new alternative sorbents is needed.

Keywords: CO_2 capture, solid adsorbent, VPSA pilot-scale unit.

1. Introduction

Reducing carbon dioxide (CO_2) emissions is a critical challenge in preventing global warming and climate change. The development of efficient technologies for CO_2 capture from industrial emissions is, therefore, a subject of intense research. Vacuum Pressure Swing Adsorption (VPSA) is emerging as one of the promising methods due to its ability to effectively capture CO_2 by adsorption on solid sorbents [1].

The VPSA method offers several significant advantages over conventional technologies, such as chemical absorption or cryogenic separation. The main benefits include lower energy consumption, higher selectivity and capture efficiency, and the possibility of repeated sorbent regeneration. A key factor for the successful implementation of VPSA technology is a detailed understanding of adsorption isotherms, which describe the relationship between pressure, temperature, and the amount of CO_2 adsorbed on the surface of the adsorbent [2].

This paper provides a comprehensive overview of the VPSA method, starting with the theoretical basis of adsorption isotherms, through the construction and optimisation of a laboratory VPSA unit, to the analysis of the results of initial experimental measurements. Data from these experimental measurements are compared with theoretical models of adsorption isotherms to evaluate the accuracy and efficiency of the VPSA technology in real-world conditions.

1.1. Adsorption

Carbon capture and storage (CCS) technologies include methods for reducing CO_2 emissions primarily from fossil fuel combustion, but they are also applicable in industries, such as cement production, metallurgy, and petrochemicals. These technologies are critical for mitigating greenhouse gas emissions and combating climate change. CCS methods can be categorised as post-combustion, where CO_2 is captured from flue gases after combustion, requiring high flue gas purity to avoid sorbent contamination; pre-combustion, where CO_2 is captured before combustion, often through processes such as coal gasification; and oxyfuel, where the fuel is burned in a controlled oxygen environment, producing flue gases consisting mainly of CO_2 and water vapour, which can be easily separated after condensation [3].

Carbon capture methods are summarised in Figure 1.

This article focuses on the post-combustion CO_2 capture methods, specifically adsorption, where CO_2 is captured using solid sorbents. The principle of CO_2 capture by adsorption is very similar to absorption. Like absorption, adsorption can be divided into physical (using weak Van der Waals forces) and chemical. The adsorption process can take place under different pressure and temperature conditions. Over the years, considerable efforts have been devoted to developing solid sorbents, but much less to the development of adsorption units, especially continu-

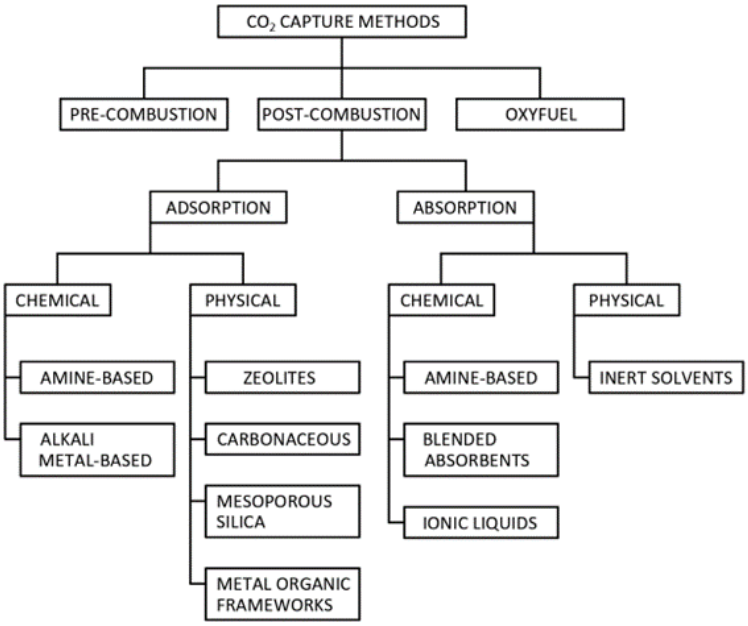

Figure 1. CO_2 capture methods.

ous adsorption units. In addition, most of the tests have been carried out with synthetic flue gases (a gas mixture of 15 % CO_2 and 85 % N_2) [4].

Depending on the adsorption and regeneration methods, processes can be categorised as follows:

- pressure swing adsorption (PSA),
- temperature swing adsorption (TSA).

Special cases of PSA and TSA processes are Vacuum Pressure Swing Adsorption (VPSA) and Vacuum Temperature Swing Adsorption [5, 6].

1.1.1. PSA

Carbon dioxide is adsorbed on the surface of particles under high pressure. By reducing the pressure around the adsorbent, the effect of the force is reduced, and carbon dioxide is released from the adsorbent's surface. The pressure difference between adsorption and desorption phases can reach up to several MPa [7, 8].

1.1.2. TSA

Adsorption and desorption are achieved by changing the temperature. The adsorption process takes place at normal ambient temperatures, and increasing the temperature in the reactor increases the kinetic energy of the captured molecules, releasing the adsorbed gas. The desorption process typically takes place at temperatures around 120–250 °C. Although the desorption process takes longer than the adsorption process, it achieves a higher purity of the output gas, up to 95 %, compared to approximately 85 % for PSA [6].

1.1.3. VPSA

The VPSA process consists of several cyclic phases: adsorption, desorption, sorbent regeneration, and evacuation. This process is energy-efficient and suitable for industrial applications due to its flexibility and high efficiency. VPSA technology operates on cyclic pressure fluctuations, allowing the sorbent to repeatedly adsorb and desorb CO_2. During the adsorption phase, the gas mixture is passed through a vessel filled with a solid sorbent at elevated pressure, where CO_2 is selectively adsorbed onto the sorbent's surface. The other gases that are not captured are vented away. After the sorbent is saturated with CO_2, the desorption phase follows, during which the pressure is reduced to below atmospheric pressure (vacuum), releasing the adsorbed CO_2. This step allows efficient sorbent regeneration and its reuse in the next cycle. The vacuum phase is crucial for reducing the overall energy consumption of the process, as it allows CO_2 to be removed with lower energy requirements compared to conventional methods [9, 10].

1.2. Adsorption isotherms

Adsorption isotherms play a crucial role in the design and optimisation of VPSA processes by expressing the relationship between adsorption capacity and the partial pressure of the adsorbate at constant temperature, where the adsorbed amount increases with increasing partial pressure. Commonly used adsorption isotherm models, such as Langmuir and Freundlich isotherms, provide a theoretical framework for interpreting the experimental data [11, 12].

Adsorption isotherms are mathematical equations that describe the relationship between specific surface excess and pressure, offering insights into the nature of the adsorbent, adsorption mechanism, and equilibrium parameters such as equilibrium adsorption capacity. As pore size decreases, adsorption energy increases, causing micropore filling at very low pressures and distorting the lowest part of the adsorption isotherm [13].

The Langmuir adsorption isotherm is a widely used model that describes the adsorption of molecules on a solid surface, forming a monolayer. The mathematical equation for the Langmuir isotherm is given by equation:

$$a_e = a_{\max} \frac{bp_i}{1 + bp_i}, \tag{1}$$

where

a_e is the amount of adsorbed gas at partial pressure of the adsorbate p_i,

$a_{\max}$ is the maximum amount of gas required to cover the surface with monolayer,

b represents the ratio of the adsorption and desorption constants, where $b = b(T)$.

This equation assumes that adsorption takes place at specific homogeneous sites within the adsorbent, and that once a site is occupied, no further adsorption can take place at that site, reflecting a monolayer adsorption process [12].

Figure 2 shows the theoretical shape of the Langmuir adsorption isotherm. The steepness and form depend on the ratio of the adsorption and desorption constants b at constant temperature T. The surface coverage θ and the equilibrium capacity a_e depend on the temperature T at which the adsorption process takes place [13].

This fundamental equation of surface chemistry underlies the B. E. T. theory, which describes multilayer adsorption and is the most important theory of physical adsorption. Langmuir derived the adsorption isotherm equation using a kinetic model and the concept of dynamic equilibrium, based on assumptions that the adsorbent surface has a fixed number of energetically equivalent adsorption sites, adsorption takes place in a monolayer, and equilibrium is reached when the adsorption and desorption rates are equal [12, 14].

Comparing theoretical isotherms with the experimental data from the pilot-scale VPSA unit verifies these models and enhances the accuracy of predictions for sorbent behaviour in real conditions.

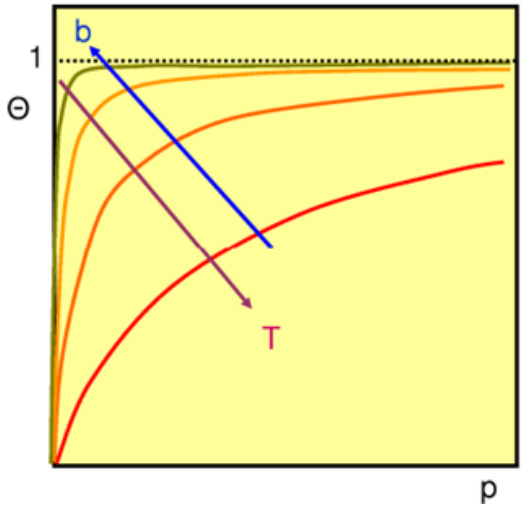

FIGURE 2. Theoretical shape of the Langmuir adsorption isotherm [13].

2. Experimental setup

2.1. Pilot-scale VPSA unit

The experimental adsorption unit consists of several key components: flue gas treatment, adsorption reactors, and a vacuum pump. Prior to the adsorption process, the flue gases from the boiler are cleaned of solid pollutants in a two-stage cleaning process: first in a cyclone separator and then in a fabric filter to further reduce the particulate content. The cleaned flue gases are then routed through two plate heat exchangers to significantly reduce moisture via condensation and cool them to the required temperature. These heat exchangers operate in a counter-flow configuration, with the first using water at approximately 15 °C and the second connected to a recirculating chiller using ethylene glycol, cooling the gases to approximately 5 °C. Both heat exchangers have a condensate drain. The processed gases are then compressed.

The adsorbent used in this pilot test, molecular sieve 13X, is highly sensitive to moisture contamination, which drastically reduces its adsorption capacity and efficiency. If CO_2 capture is to be carried out on flue gases from fuels other than biomass, additional cleaning to remove acidic components and heavy metals is necessary. For this experiment, wood pellets without sulphur or heavy metals were used.

The cooled, dehumidified flue gases are compressed to approximately 8 bar using a screw compressor. The pressure is regulated to 5 bar(g), the operational pressure of the VPSA unit, via a control valve. After the compressor, another condensate separator removes the residual water. The design flow rate for flue gases entering the adsorption reactors is between 5–50 $m^3_N\,h^{-1}$ at approximately 5 °C.

Figure 3 is a photograph of the laboratory adsorption unit with labelled components. The unit consists of three parallel columns, allowing simultaneous adsorption, desorption, and sorbent regeneration processes. The adsorption columns are made of stainless steel cylinders, DN 200 PN 10. Both the top and bottom flanges are equipped with conical screens to prevent the loss of the adsorbent material and to improve the distribution of flue gases inside the reactor. Figure 4 shows a piping and instrumentation diagram of the described pilot-scale adsorption unit.

In the adsorption unit, thermocouples were strategically placed within the reactor to monitor temperature distribution during the adsorption. These thermocouples were positioned approximately 400 mm apart along the length of the reactor, providing detailed thermal profiling at multiple points. The placement of the thermocouples enabled the detection of temperature gradients and localised heating within the adsorption bed, which are critical for understanding

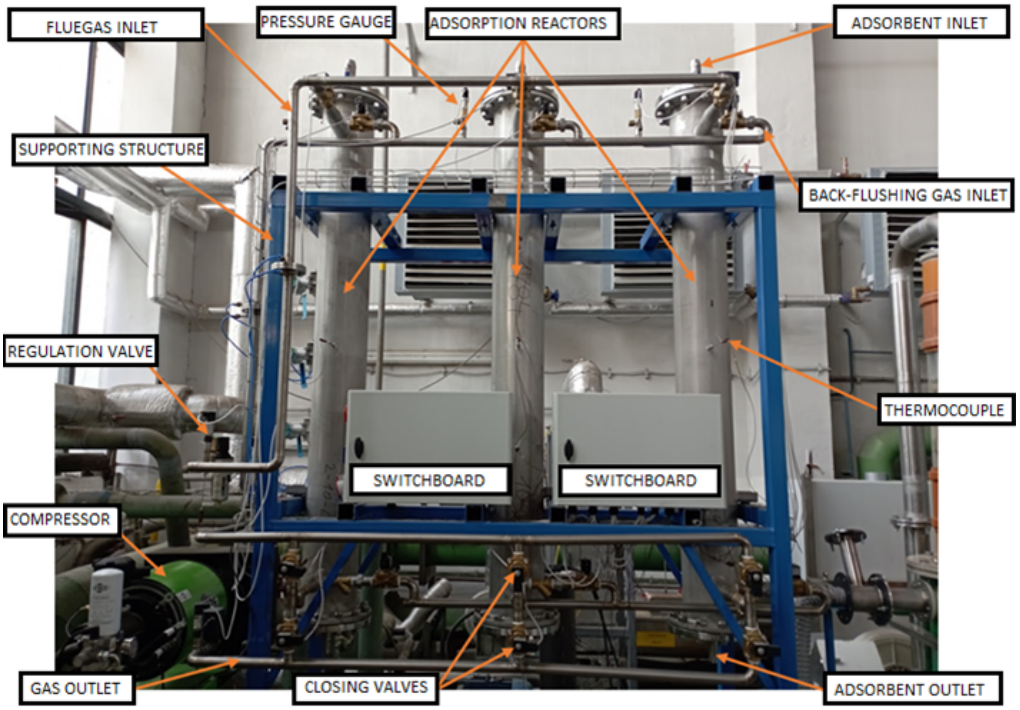

Figure 3. Photography of the adsorption pilot-scale unit.

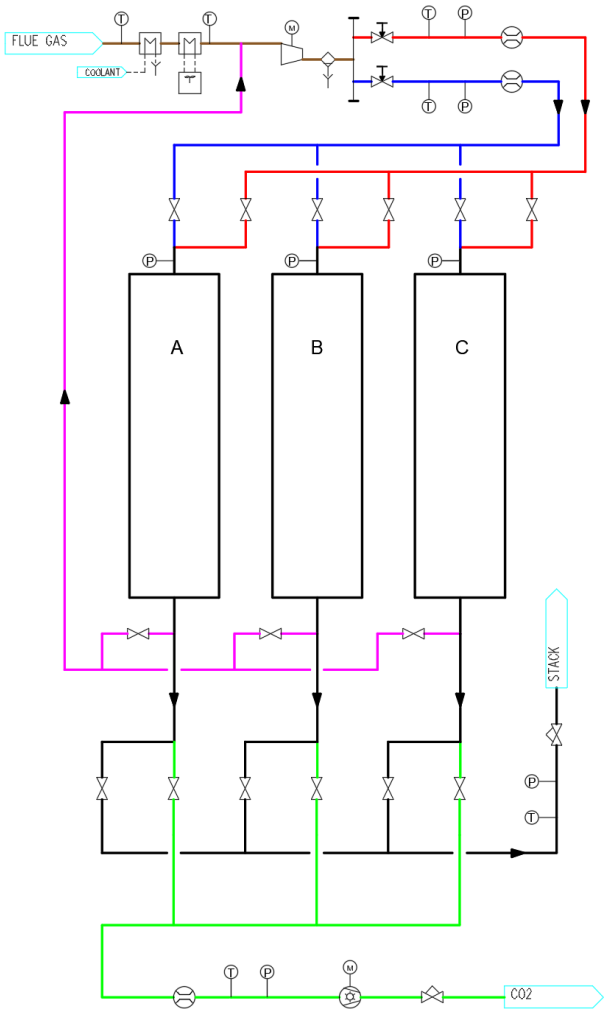

Figure 4. Piping and instrumentation diagram of the pilot-scale unit.

the exothermic nature of the adsorption process and its impact on the overall performance and efficiency of the reactor. The data collected from these thermocouples are essential for evaluating the thermal behaviour of the sorbent and optimising process conditions to achieve consistent adsorption performance.

The PID (Piping and Instrumentation Diagram), shown in Figure 4, illustrates the configuration of the adsorption unit. The diagram shows two inlet and three outlet branches for each column, with individual paths differentiated by colour. The blue section, labelled as the "pressurisation" path, directs the flue gases through a pressure-reducing valve, adjusting the pressure to a maximum of 5 bar before entering the column. The green path, referred to as the "rich", is used during the desorption phase. When the desorption begins, the column's outlet valve opens, allowing the adsorbed gas to be evacuated under vacuum created by a vacuum-pump. The desorbed gas is then analysed, providing key data on the adsorption cycle's efficiency. The red path is designated for the regeneration of the sorbent using air. During the regeneration, air flows through the column at atmospheric pressure, flushing out the remaining CO_2 and regenerating the adsorbent material, preparing it for the next adsorption cycle. The purple path is intended for the recirculation of flue gases during the sorbent regeneration, directing the gases back to the compressor for reuse in the adsorption process. However, in the current setup, the regeneration is performed using air.

This setup ensures efficient operation and control of the adsorption, desorption, and regeneration processes within the adsorption unit, as shown in Figure 4.

Adsorbent	Temperature [K]	Pressure [bar]	CO_2 adsorption capacity [mmol g^{-1}]
Zeolite 4A	298	1	2.20
Zeolite 5A	298	1	3.68
Zeolite 13X (13X-C)	298	1	6.20
Zeolite 13X (13X-B)	298	1	4.80

TABLE 1. CO_2 sorption capacities of zeolite variants [15].

Description	Unit	Value
Sorbent	-	Zeolite 13X
Shape of the particles	-	Spherical
Adsorption capacity	mmol g^{-1}	2.6
Particle diameter	mm	1.9 to 2.1
Particle volume	mm^3	3.59 to 4.85
Density	kg m^{-3}	710 to 730
Porosity	-	0.373
Effective pore size	nm	1

TABLE 2. Properties of used sorbent Zeolite 13X.

2.2. SORBENT

In this test, industrially applicable zeolite 13X was used as the sorbent to evaluate the functionality of the laboratory unit. Zeolites are natural or synthetic aluminosilicates that have channels and cavities of precisely defined dimensions and shapes within their crystalline structure [16].

Zeolites with low Si content are categorised into three main types according to the Si/Al ratio. A molar ratio of Si/Al equal to 1 defines zeolite type A. A ratio between 1 and 1.5 defines zeolite type X, and a ratio greater than 1.5 defines zeolite type Y. In all cases, the molar fraction of Al in the zeolite must be at least 0.5. Zeolites have a strongly hydrophilic character, making their adsorption capacity for CO_2 highly dependent on the concentration of water vapour. Zeolites are influenced more by polar and electrostatic forces than by Van der Waals forces. Similarly to carbonaceous materials, zeolites can be impregnated with other elements to increase adsorption capacity or selectivity for CO_2 (these materials are under development and some will be tested in the future in another pilot-scale unit). Adsorption using zeolites occurs at lower temperatures and typically also at lower pressures, which is why desorption usually involves vacuum methods. The adsorption capacity of pure zeolites typically ranges from 1 to 6 mmol g^{-1} [17, 18].

Table 1 shows the CO_2 sorption capacities of zeolites 13X (variants 13X-C and 13X-B), 4A, and 5A. The data provide a comparative overview of each zeolite's CO_2 adsorption efficiency under consistent constant conditions, allowing a basic evaluation of their relative performance. This comparison highlights variations in structural properties that influence sorption capacities [15].

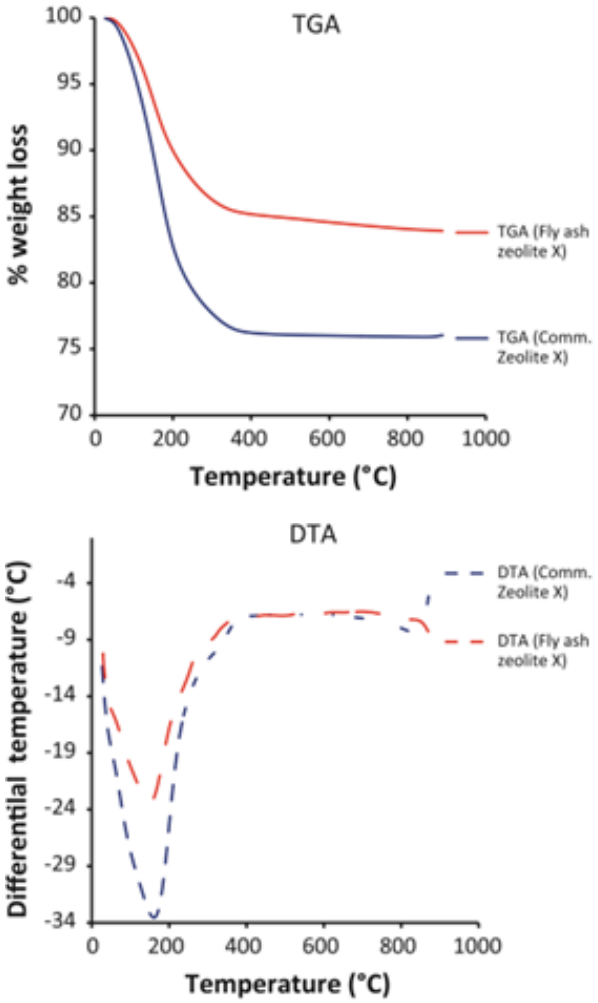

FIGURE 5. Comparative TGA-DTA curves of zeolites [19].

The properties of the sorbent used in the test are presented in Table 2.

Figure 5 presents the TGA and DTA curves for commercial zeolite 13X and zeolite synthesized from coal fly ash. As shown in Figure 5, the TGA curve indicates desorption of physically adsorbed water within the micropores. The weight losses of approximately 15 % for the fly ash based Zeolite X and 25 % for the commercial Zeolite X. This significant weight loss, occurring in the temperature range of 50–400 °C for both zeolites, corresponds to the release of free and physically adsorbed water from within the pores. The weight loss stabilises at approximately 400 °C, reflecting the completion of water desorption [19].

Description	Unit	Value
Sorbent	-	Zeolite 13X
Amount of the sorbent	kg	46.0
Volumetric CO_2 concentration of wet flue gas	-	0.1044
Operating mode of the unit	-	Flow-through
Flue gas temperature – inlet	°C	5
Flue gas pressure in reactor	kPa	500
Flue gas flow	$m^3_N\,h^{-1}$	8–14

Table 3. Conditions of the experiment.

Properties as received	Unit	Value
C	wt. %	45.83
H	wt. %	6.71
S	wt. %	<0.003
N	wt. %	0.03
O	wt. %	39.72
Cl	wt. %	<0.0005
Water	wt. %	7.32
Ash	wt. %	0.40
LHV	$MJ\,kg^{-1}$	16.09

Table 4. Analysis of fuel used in boiler for experiments.

The sorbent used in the test was dried at 180 °C for approximately 24 hours to remove any residual moisture. This pre-treatment step was essential to ensure optimum adsorption performance by minimising the impact of humidity on the sorbent's capacity. However, considering Figure 5, it is evident that the treatment of the sorbent used in the tests was insufficient to remove most of the residual moisture and should be dried at higher temperatures (at least 380 °C).

2.3. Used fuel

For the tests, wooden pellets were chosen as the fuel. These pellets, a type of biofuel, typically have a diameter of 6–8 mm. The advantages of this fuel include high calorific value due to its homogeneity, low moisture content, low ash content, and low levels of sulphur and heavy metals, which can contaminate the sorbent. The essential properties of the fuel used are provided in Table 4.

2.4. Methodology

The test was carried out with the experimental pilot-scale unit described above to verify the capabilities of Zeolite 13X in real conditions (using real flue gas from the boiler). The test was performed under the following conditions listed in Table 3.

For the experimental measurements, only column "B" was filled with sorbent. This column is equipped with thermocouples to monitor temperature changes inside the reactor during adsorption, desorption, and regeneration. Three adsorption-desorption cycles were carried out with a single batch of sorbent, with volumetric flow rates recorded from the rotameter for each cycle. The first two cycles were carried out with a flue gas flow rate of approximately $8\,m^3_N\,h^{-1}$, while the third cycle was performed with a higher flow rate in the range of 13–14 $m^3_N\,h^{-1}$. The primary focus of this experiment was on the adsorption phase, where the adsorption characteristics of the material were thoroughly investigated. While the desorption and regeneration phases were conducted as part of the overall experimental process, the data and findings from these phases were not included in the analysis and are not discussed within the scope of this paper. The results presented here exclusively pertain to the adsorption phase, with subsequent phases reserved for future studies.

3. Results and discussion

This chapter presents the results obtained during the initial experimental measurements on the laboratory VPSA unit using zeolite 13X as a solid sorbent. The results include the measurement of CO_2 capture efficiency and the comparison of theoretical models with experimental data. CO_2 concentration values and excess oxygen (O_2) in the flue gas were obtained from analysers placed after the boiler, which were recalculated to air excess values. These values were averaged only during the adsorption period. The adsorption pressure was read from the pressure gauges on the reactor, averaged, and used to calculate the partial pressure of CO_2 in the flue gas. All of the mentioned input parameters of the measurements are listed in Table 5.

Subsequently, breakthrough curves were established from the measured values. Figure 6 shows the breakthrough curves, which illustrate the relationship between the CO_2 outlet concentration and time.

At the beginning of the measurement, the CO_2 outlet concentration was not zero as shown in Figure 6, which was attributed to the residual volume of flue gas that had accumulated in the piping system behind the reactor before the CO_2 analyser. Figure 6 shows that the adsorption time is directly dependent on the gas flow rate, with the first two cycles performed at the same flow rate, exhibiting very similar trends and times to reach a stable CO_2 outlet concentration.

Description	Unit	Value		
Cycle		1	2	3
Excess oxygen in flue gas	%	7.223	7.903	7.412
Air excess	-	1.524	1.603	1.545
Concentration of CO_2 in flue gas	%	12.207	11.516	11.987
Flue gas flow	$m^3_N\,h^{-1}$	8	8	13.5
Average adsorption pressure in reactor	kPa	393.7	391.8	387.3
Partial pressure of CO_2	kPa	48.1	45.1	46.4
Average temperature in reactor	°C	28.78	28.29	27.62

TABLE 5. Measured values.

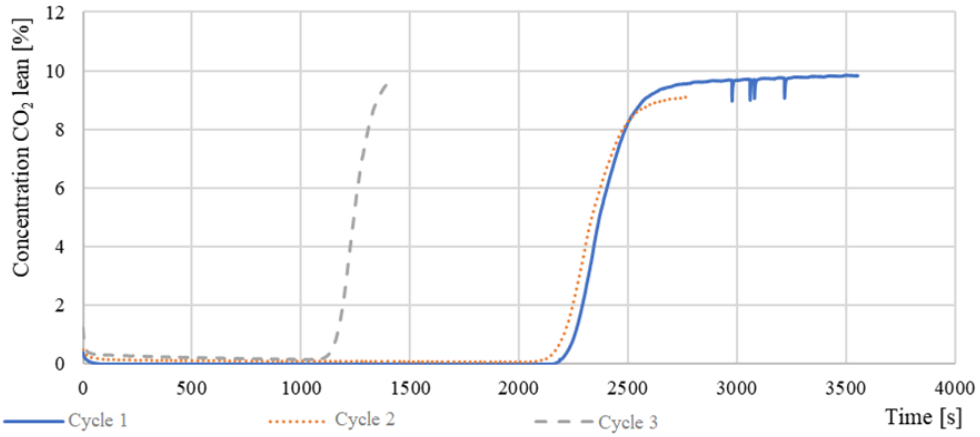

FIGURE 6. Breakthrough curves of each cycle.

The slight difference observed in Cycle 2 compared to Cycle 1 can be attributed to variations in CO_2 concentration in the flue gas, incomplete desorption from Cycle 1, or contamination of the sorbent with residual moisture from Cycle 1. Cycle 3, with a higher flow rate, shows a significantly reduced breakthrough time and a steeper increase in CO_2 concentration at the outlet compared to the previous two cycles.

Figure 7 illustrates the temperature distribution within the reactor during the first cycle of the adsorption process, with the graph depicting temperature changes over time.

The data revealed a noticeable temperature increase shortly after the initiation of the adsorption phase, indicating the exothermic nature of CO_2 capture by the zeolite sorbent. As the cycle progresses, the temperature reaches a peak before gradually stabilising, reflecting the equilibrium between heat generation and dissipation within the reactor. The temperature distribution is not uniform along the reactor length, likely due to the gradual saturation of the sorbent as the gas flows through the reactor. This variation in temperature suggests that different sections of the sorbent bed reach saturation at different times, affecting the overall adsorption efficiency. Thermocouple T1B is positioned at the topmost section of the reactor, with each subsequent thermocouple positioned progressively downwards along the reactor length. The thermocouples are spaced approximately 400 mm apart, capturing the temperature distribution throughout the sorbent bed. Thermocouple TB1, which was not in direct contact with the sorbent, showed minimal temperature variation on the graph, remaining nearly constant throughout the experiment. These insights emphasise the importance of thermal management and uniform sorbent utilisation in optimising the performance of the VPSA unit.

From the measured values, including the known gas flow rate, CO_2 concentration at the column inlet, and adsorption time, the amount of captured adsorbate per cycle was determined by using equation:

$$m_{CO_2} = \dot{V}_{\text{fluegas}} \cdot \varphi_{CO_2 IN} \cdot \rho_{CO_2} \cdot \text{time}. \qquad (2)$$

This mass is compared in Table 6 with the theoretical mass computed for the input conditions of the actual experiment. The equilibrium capacity closest to the average temperature in the adsorber, as shown in Figure 8, was derived from the adsorption isotherm. The adsorption isotherms used in this study were obtained from the master's thesis [20], providing essential data for validating the theoretical models and enhancing the accuracy of the adsorption process analysis. The mass of the sorbent in the reactor is assumed to be identical for both experimental measurements and theoretical calculations.

The results of the initial experimental measurements on the VPSA unit, as presented in Table 6, reveal some interesting insights when compared with the theoretical predictions. Despite using established

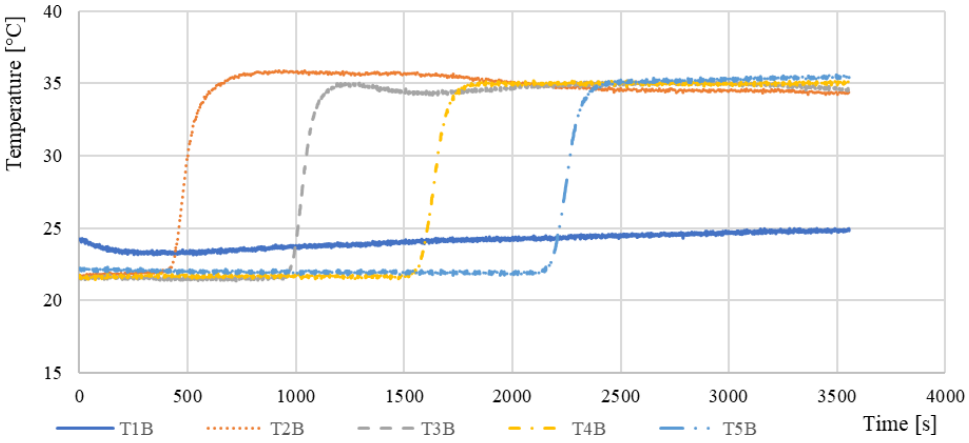

Figure 7. Temperature inside reactor during Cycle 1.

Description	Unit	Value		
Cycle		1	2	3
Used adsorption isotherm	°C	30	30	30
Partial pressure of CO_2 (sorption)	kPa	48.1	45.1	46.4
Partial pressure of CO_2 (desorption)	kPa	5.11	5.11	5.11
Adsorption capacity of CO_2	$g\,g^{-1}$	0.06196	0.06037	0.05888
Theoretical weight of captured of CO_2	kg	2.85	2.78	2.71
Actual volume of captured CO_2	Nm^3	0.712	0.616	0.563
Actual mass of captured CO_2	kg	1.389	1.202	1.098

Table 6. Comparison of theoretical and experimental values.

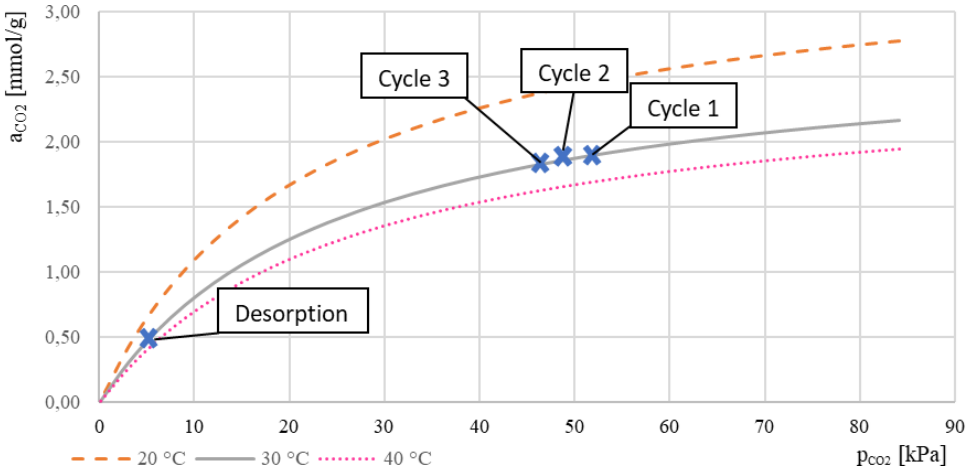

Figure 8. Dependence of Zeolite 13X capacity on partial pressure.

adsorption isotherms to estimate the CO_2 capture capacity, the actual experimental data consistently showed lower captured CO_2 mass for all cycles. For example, in Cycle 1, the theoretical mass of CO_2 captured was 2.85 kg, but the actual measured mass was only 1.389 kg. Similar trends were observed in Cycles 2 and 3, with the experimental values falling short of the theoretical predictions. This discrepancy suggests that while the theoretical models provide a useful baseline, they may not fully capture the complexities of the real-world adsorption process in the VPSA unit.

One key factor contributing to the difference between theoretical and experimental results could be the non-uniform temperature distribution within the reactor, as evidenced by the data shown in Figure 7. The temperature variations along the reactor length likely influenced the adsorption efficiency, as different sections of the sorbent bed reached saturation at different times. In addition, the presence of residual moisture in the sorbent and incomplete desorption between cycles, may have further reduced the adsorption capacity. These factors, combined with the potential limitations in process control during the experiments, underscore the challenges of translating theoretical models into practical applications.

4. Conclusion

Table 6 reveals that the experimental values carried out on the pilot-scale adsorption unit did not confirm the values predicted by the theoretical model. Initial tests showed significant discrepancies between the results from the models and the data obtained from the first experimental trials. These differences may be due to assumptions of ideal processes in theoretical model versus actual operational conditions, non-optimised control of the adsorption process, or failure to reach adsorption equilibrium.

It is possible that the drying of the sorbent at 180 °C was not sufficient, and it may be necessary to dry the sorbent at higher temperatures, around 380 °C. Looking at Figure 5, it is evident that the treatment of the sorbent used in the tests was insufficient to remove most of the residual moisture. This insufficient drying could be a contributing factor to the difference observed between the theoretical model and the measured values. It is important to note that handling the sorbent after drying could affect the results by allowing it to reabsorb atmospheric moisture, potentially impacting its measured CO_2 sorption capacity.

For integration of the adsorption unit into real flue gas cleaning operations, it is ideal to terminate adsorption at the breakthrough time to prevent CO_2 from passing through the column without capture. It is evident that the maximum sorbent capacity would only be used if an equilibrium is reached, where the CO_2 concentrations at the outlet and inlet are equal.

The experimental measurements confirmed that maintaining a low, constant temperature in the columns during the actual operation is not feasible without external cooling. This means that the adsorption and desorption processes do not follow ideal adsorption isotherms, leading to lower amounts of captured adsorbate than in an ideal scenario. This is due to the exothermic nature of adsorption, which releases heat and warms the adsorption reactor.

List of symbols

a Adsorption capacity $[\mathrm{mmol\,g^{-1}}]$
m Mass [kg]
p Pressure [kPa]
φ Concetration [%]
Q Flow $[\mathrm{m^3_N\,h^{-1}}]$
ρ Density $[\mathrm{kg\,m^{-3}}]$
$\dot{V}$ Flow rate $[\mathrm{m^3\,h^{-1}}]$
CO_2 Carbon dioxide

Acknowledgements

This work was supported by SGS Grant from CTU FSI: 161-1612311B001, which is gratefully acknowledged.

References

[1] M. E. Boot-Handford, J. C. Abanades, E. J. Anthony, et al. Carbon capture and storage update. *Energy & Environmental Science* **7**(1):130–189, 2014. https://doi.org/10.1039/c3ee42350f

[2] C. Shen, Z. Liu, P. Li, J. Yu. Two-stage VPSA process for CO_2 capture from flue gas using activated carbon beads. *Industrial & Engineering Chemistry Research* **51**(13):5011–5021, 2012. https://doi.org/10.1021/ie202097y

[3] C. Song. Global challenges and strategies for control, conversion and utilization of CO_2 for sustainable development involving energy, catalysis, adsorption and chemical processing. *Catalysis Today* **115**(1–4):2–32, 2006. https://doi.org/10.1016/j.cattod.2006.02.029

[4] S. Choi, J. H. Drese, C. W. Jones. Adsorbent materials for carbon dioxide capture from large anthropogenic point sources. *ChemSusChem* **2**(9):796–854, 2009. https://doi.org/10.1002/cssc.200900036

[5] L. Wang, Z. Liu, P. Li, et al. Experimental and modeling investigation on post-combustion carbon dioxide capture using zeolite 13X-APG by hybrid VTSA process. *Chemical Engineering Journal* **197**:151–161, 2012. https://doi.org/10.1016/j.cej.2012.05.017

[6] N. Jiang, Y. Shen, B. Liu, et al. CO_2 capture from dry flue gas by means of VPSA, TSA and TVSA. *Journal of CO_2 Utilization* **35**:153–168, 2020. https://doi.org/10.1016/j.jcou.2019.09.012

[7] I. Durán, F. Rubiera, C. Pevida. Modeling a biogas upgrading PSA unit with a sustainable activated carbon derived from pine sawdust. Sensitivity analysis on the adsorption of CO_2 and CH_4 mixtures. *Chemical Engineering Journal* **428**:132564, 2022. https://doi.org/10.1016/j.cej.2021.132564

[8] L. Riboldi, O. Bolland. Overview on pressure swing adsorption (PSA) as CO_2 capture technology: State-of-the-art, limits and potentials. *Energy Procedia* **114**:2390–2400, 2017. https://doi.org/10.1016/j.egypro.2017.03.1385

[9] D. M. Ruthven, S. Farooq, K. S. Knaebel. *Pressure swing absorption*. Wiley-VCH Verlag, Germany, 1993. ISBN 9783527895175.

[10] D. M. Ruthven. *Principles of adsorption and adsorption processes*. John Wiley & Sons, 1984.

[11] F. G. Helfferich. Principles of adsorption & adsorption processes. *AIChE Journal* **31**(3):523–524, 1985. https://doi.org/10.1002/aic.690310335

[12] H. Swenson, N. P. Stadie. Langmuir's theory of adsorption: A centennial review. *Langmuir* **35**(16):5409–5426, 2019. https://doi.org/10.1021/acs.langmuir.9b00154

[13] R. Bulánek. *Povrchové jevy na pevných látkách [In Czech; Surface phenomena on solid substances]*. Univerzita Pardubice, 2015. ISBN 9788073959081.

[14] A. Samanta, A. Zhao, G. K. H. Shimizu, et al. Post-combustion CO_2 capture using solid sorbents: A review. *Industrial & Engineering Chemistry Research* **51**(4):1438–1463, 2011. https://doi.org/10.1021/ie200686q

[15] F. Bahmanzadegan, A. Ghaemi. Modification and functionalization of zeolites to improve the efficiency of CO_2 adsorption: A review. *Case Studies in Chemical and Environmental Engineering* **9**:100564, 2024. https://doi.org/10.1016/j.cscee.2023.100564

[16] C. Martínez Sánchez, J. Pérez-Pariente. *Zeolites and ordered porous solids: Fundamentals and applications*. Universitat Politècnica de Valencia, 2011. ISBN 9788483637197.

[17] Y. Jiang, J. Ling, P. Xiao, et al. Simultaneous biogas purification and CO_2 capture by vacuum swing adsorption using zeolite NaUSY. *Chemical Engineering Journal* **334**:2593–2602, 2018. https://doi.org/10.1016/j.cej.2017.11.090

[18] S. M. W. Wilson. High purity CO_2 from direct air capture using a single TVSA cycle with Na-X zeolites. *Separation and Purification Technology* **294**:121186, 2022. https://doi.org/10.1016/j.seppur.2022.121186

[19] N. M. Musyoka, L. F. Petrik, E. Hums, et al. Thermal stability studies of zeolites A and X synthesized from South African coal fly ash. *Research on Chemical Intermediates* **41**(2):575–582, 2013. https://doi.org/10.1007/s11164-013-1211-3

[20] J. Burda. *Záchyt oxidu uhličitého pomocí VPSA adsorpčního cyklu [In Czech; Carbon dioxide capture by VPSA cycle]*. Master's thesis, Czech Technical University in Prague, Faculty of Mechanical Engineering, 2024.